LAWRENCE
LIVERMORE
NATIONAL
LABORATORY

LLNL-CONF-563732

Improving the J/psi Production Baseline at RHIC and the LHC

R. Vogt, R. E. Nelson, A. D. Frawley

July 10, 2012

Hard Probes 2012
Cagliari, Italy
May 28, 2012 through June 1, 2012

Disclaimer

This document was prepared as an account of work sponsored by an agency of the United States government. Neither the United States government nor Lawrence Livermore National Security, LLC, nor any of their employees makes any warranty, expressed or implied, or assumes any legal liability or responsibility for the accuracy, completeness, or usefulness of any information, apparatus, product, or process disclosed, or represents that its use would not infringe privately owned rights. Reference herein to any specific commercial product, process, or service by trade name, trademark, manufacturer, or otherwise does not necessarily constitute or imply its endorsement, recommendation, or favoring by the United States government or Lawrence Livermore National Security, LLC. The views and opinions of authors expressed herein do not necessarily state or reflect those of the United States government or Lawrence Livermore National Security, LLC, and shall not be used for advertising or product endorsement purposes.

Available online at www.sciencedirect.com
ScienceDirect
Nuclear Physics A 00 (2012) 1–4
Nuclear Physics A

Improving the J/ψ Production Baseline at RHIC and the LHC

R. Vogt[1,2], R. E. Nelson[1,2] and A. D. Frawley[3]

[1]*Lawrence Livermore National Laboratory, Livermore, CA 94550, USA*
[2]*University of California, Davis, CA 95616, USA*
[3]*Florida State University, Tallahassee, FL , USA*

Abstract

We assess the theoretical uncertainties on the inclusive J/ψ production cross section in the Color Evaporation Model using values for the charm quark mass, renormalization and factorization scales obtained from a fit to the charm production data. We use our new results to provide improved baseline comparison calculations at RHIC and the LHC. We also study cold matter effects on J/ψ production at leading relative to next-to-leading order in the CEM within this approach.

Keywords: quarkonium, cold nuclear matter

Because the charm quark mass is finite, the total charm production cross section can be calculated in perturbative QCD. However, there are large uncertainties due to the choice of quark mass, factorization scale and renormalization scale [1]. Typical lower limits of the factorization and renormalization scales are half the chosen charm quark mass [1, 2]. In this case, the factorization scale is below the minimum scale of the parton densities. In addition, for renormalization scales below 1 GeV, the strong coupling constant α_s becomes large and the perturbative expansion is unlikely to converge. Thus we seek a set of physically defensible mass and scale parameters that reduce the cross section uncertainty. Because the J/ψ cross sections are calculated with the same set of mass and scale parameters as open charm production in the color evaporation model [3], we also place limits on the J/ψ cross section calculated in the color evaporation model for the first time.

The uncertainties from the mass and scale variations were then added in quadrature. The envelope containing the resulting curves,

$$\sigma_{\rm max} = \sigma_{\rm cent} + \sqrt{(\sigma_{\mu,\rm max} - \sigma_{\rm cent})^2 + (\sigma_{m,\rm max} - \sigma_{\rm cent})^2}\ , \quad (1)$$

$$\sigma_{\rm min} = \sigma_{\rm cent} - \sqrt{(\sigma_{\mu,\rm min} - \sigma_{\rm cent})^2 + (\sigma_{m,\rm min} - \sigma_{\rm cent})^2}\ , \quad (2)$$

defines the uncertainty on the total cross section as a function of center of mass energy. The charm quark mass we employ in our calculations is the Particle Data Group (PDG) value based on lattice determinations of the charm quark mass in the $\overline{\rm MS}$ scheme at $\mu = m$: $m(m) = 1.27 \pm 0.09$ GeV [4]. We fit the factorization and renormalization scale parameters to a subset of the fixed target total charm production data with $250 \le E_{\rm beam} \le 920$ GeV. The data were evaluated and adjusted to the values we employ in our fits using the most up-to-date branching ratios for the measured decay channels in Ref. [5]. We also include data from both PHENIX [6] and STAR [7, 8]. We neglect unknown next-order uncertainties which could be large for charm where the mass is relatively small and $O(\alpha_s^4)$ corrections could be significant.

The best fit, including the STAR data presented at Quark Matter 2011 [7], $m_c = 1.27$ GeV, $\mu_F/m = 2.1^{+2.55}_{-0.85}$ and $\mu_R/m = 1.6^{+0.11}_{-0.12}$. We show the χ^2/dof fit contours on the left-hand side of Fig. 1 for $\Delta\chi^2/\text{dof} = 0.3$, 1 and 2.3. The one standard deviation uncertainty in the fitted value of μ_F/m (μ_R/m) was taken as the maximum extent of the $\Delta\chi^2/\text{dof} = 1$ contour along the μ_F/m (μ_R/m) axis. The one standard deviation uncertainty in the total cross section is the range of cross sections resulting from all combinations of μ_F/m and μ_R/m contained within the $\Delta\chi^2/\text{dof} = 2.3$ contour. The $\Delta\chi^2/\text{dof} = 0.3$ contour is to guide the eye. Note the narrow range in μ_R/m relative to the much broader μ_F/m range. The uncertainty on μ_F/m is larger and very asymmetric. There is a greater uncertainty on the upper limit than the lower limit because there is a much greater change in $xg(x, \mu_F^2)$ at lower factorization scales than when $\mu_F \gg \mu_0$, the minimum scale of the parton densities.

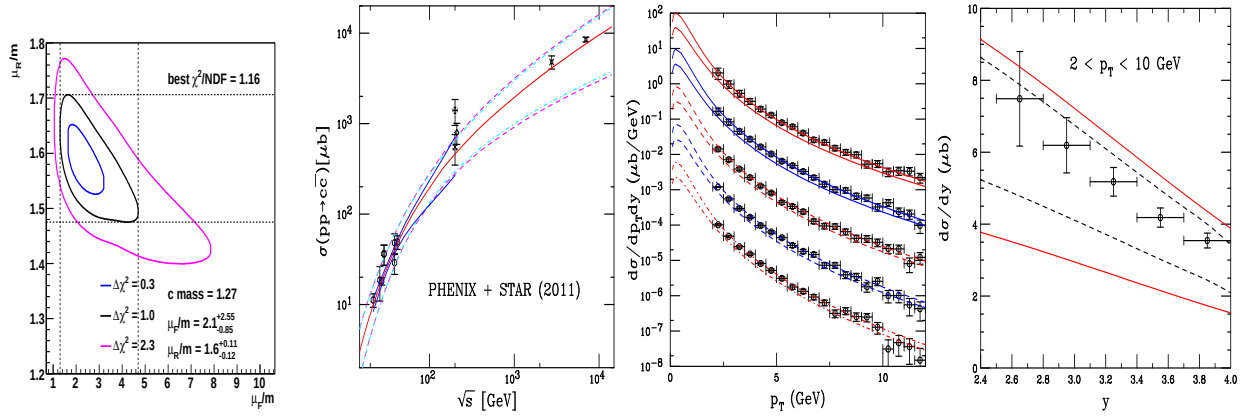

Figure 1: (First) The χ^2/dof contours for a fit to the fixed target data and the PHENIX and STAR 2011 cross sections at $\sqrt{s} = 200$ GeV. The best fit values are given for the furthest extent of the $\Delta\chi^2 = 1$ contours. (Second) The energy dependence of the charm total cross section compared to data. The best fit values are given for the furthest extent of the $\Delta\chi^2 = 1$ contours. The central value of the fit is given by the solid red curve while the dashed magenta curves and dot-dashed cyan curves show the extent of the corresponding uncertainty bands. The solid blue curves in the range $19.4 \leq \sqrt{s} \leq 200$ GeV represent the uncertainty obtained from the extent of the $\Delta\chi^2 = 2.3$ contour. (Third) The contributions to the p_T distributions in (a) divided into rapidity bins, from top to bottom: $2.5 < y < 2.8$ (solid red); $2.8 < y < 3.1$ (solid blue); $3.1 < y < 3.4$ (dashed red); $3.4 < y < 3.7$ (dashed blue); and $3.7 < y < 4$ (dot-dashed red). The top curves are shown at their calculated value, the others are scaled down by successive factors of 10 to separate them. (Fourth) The sum of contributions to the rapidity distribution are compared with the FONLL set for charm (solid red) and that with $m = 1.27$ GeV (dashed black). Our calculations are compared with the ALICE inclusive single muon data from heavy flavor decays [10] at $\sqrt{s} = 7$ TeV.

The second panel of Fig. 1 shows the energy dependence of the total charm cross section for the fits with the corresponding uncertainty based on results using the one standard deviation uncertainties on the quark mass and scale parameters. If the central, upper and lower limits of $\mu_{R,F}/m$ are denoted as C, H, and L respectively, then the seven sets corresponding to the scale uncertainty are $\{(\mu_F/m, \mu_F/m)\} = \{(C, C), (H, H), (L, L), (C, L), (L, C), (C, H), (H, C)\}$. The upper and lower limits on the PDG value of the charm quark mass are 1.36 and 1.18 GeV. The uncertainty band can be obtained for the best fit sets using Eqs. (1) and (2). The uncertainty bands are shown for two cases: the regular fiducial region and including the most extreme cases $(\mu_F/m, \mu_R/m) = (H, L)$ and (L, H). The difference between the outer magenta curves, which include these extremes, and the cyan curves, which do not, is very small. Therefore, it is reasonable to neglect the extremes. We also show the result for a one standard deviation uncertainty in the total cross section obtained from the $\Delta\chi^2 = 2.3$ contour in the blue lines. We have also added the 2.76 and 7 TeV total cross sections obtained by the ALICE collaboration in pp collisions [9], not included in our fits. The calculations are in rather good agreement with the data.

We use the FONLL approach [2] to calculate the heavy flavor semileptonic decay kinematic distributions to compare to single lepton spectra which include B decays as well as D decays. The $B \to \mu$ and $B \to D \to \mu$ bands are calculated with the same fiducial set of parameters as in Ref. [2]. The $D \to \mu$ band is calculated for our best fit

[0] Using the final STAR data point [8] in the fitting changes the upper and lower limits on μ_F/m by 8% and 4% respectively, while the limits on μ_R/m change by less than 1%.

parameter set. Figure 1 compares our calculations with the ALICE single muon data in the forward rapidity region, $2.5 < y < 4$ [10]. The data are given for $2 < p_T < 12$ GeV and separated into five rapidity bins, each 0.3 units wide, as shown in the third panel of Fig. 1. The calculations agree well with the measurements over the entire p_T range. On the right-hand side of Fig. 1 we present the results as a function of rapidity integrated over the same p_T range as the data, $2 \leq p_T \leq 10$ GeV. The p_T-integrated ALICE data agree well with both calculations. The results with the fitted charm parameter set narrow the uncertainty band without sacrificing consistency with the measured data.

We now turn to a treatment of quarkonium production within this same framework. In the CEM, the quarkonium production cross section is some fraction, F_C, of all $Q\overline{Q}$ pairs below the $H\overline{H}$ threshold where H is the lowest mass heavy-flavor hadron. Our fit of F_C is based on the total cross section data with only p, Be, Li, C, and Si targets respectively. In this way, we avoid uncertainties due to ignoring any cold nuclear matter effects which are on the order of a few percent in light targets. We also restricted ourselves to the forward cross sections only.

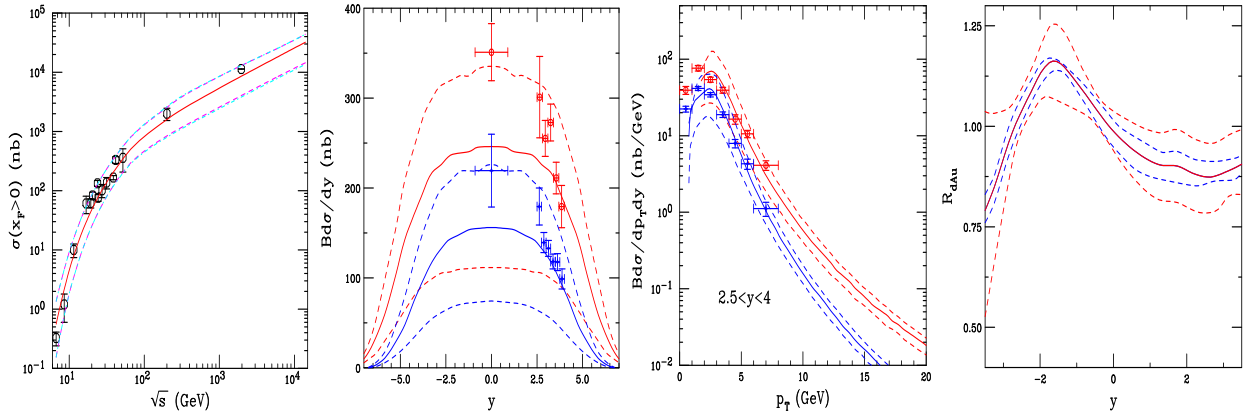

Figure 2: (First) The uncertainty band on the forward J/ψ cross section calculated based on the $c\bar{c}$ fit. The dashed magenta curves and dot-dashed cyan curves show the extent of the corresponding uncertainty bands. The dashed curves outline the most extreme limits of the band. (Second) The J/ψ rapidity distributions compared to data from 7 TeV [11] (red points and band) and 2.76 TeV [12] (blue points and band). (Third) The forward p_T distributions ($2.5 < y < 4$) are also shown. No additional scaling factor has been applied. A $\langle k_T^2 \rangle$ kick of 1.49 GeV^2 (7 TeV) and 1.41 GeV^2 (2.76 TeV) is applied to the p_T distributions. (Fourth) The scale variation of $R_{\rm dAu}$ with the central EPS09 set (blue) compared to the EPS09 variation for the central parameter set (red).

We use the same values of the central charm quark mass and scale parameters as we found for open charm to obtain the normalization F_C for $(m, \mu_F/m, \mu_R/m) = (1.27\,\text{GeV}, 2.1, 1.6)$. We determine F_C only for the central parameter set and scale all the other calculations by the same value of F_C to obtain the extent of the J/ψ uncertainty band. The result is shown on the left-hand side of Fig. 2.

The ALICE 2.76 and 7 TeV rapidity and forward p_T distributions are shown in the second and third plots of Fig. 2. The rapidity distribution at $\sqrt{s} = 7$ TeV is flat over several units of rapidity. The calculated rapidity distribution at 2.76 TeV is not as broad and the agreement with the data is rather good although the midrapidity point remains high relative to the central value of the calculation. The agreement of the calculated p_T distributions with the forward rapidity data is quite good with the exception of the lowest p_T points where the calculated distributions turn over more quickly than the data.

Finally, in the right-hand panel of Fig. 2, we show the ratio $R_{\rm dAu}$ for 200 GeV d+Au collisions at RHIC to NLO in the total cross section with EPS09 NLO shadowing. The blue band shows the variation with respect to the 31 EPS09 sets while the red band indicates the mass and scale variation around the central set. We note that, with the best fit set, the scale uncertainty is now less than the uncertainty due to shadowing.

We have narrowed the uncertainty band on the open heavy flavor cross section and, in so doing, have also provided a realistic uncertainty band on J/ψ production in the color evaporation model. The central result, $m = 1.27$ GeV, $\mu_F/m = 2.1$ and $\mu_R/m = 1.6$, is quite compatible with previous calculations using a 'by-eye' fit to the data with $m = 1.2$ GeV, $\mu_F/m = \mu_R/m = 2$ [3, 13].

While the fits have been made by comparing the calculated NLO charm production cross section to available data

at fixed-target energies and at RHIC, they are in good agreement with the extracted total charm cross sections at the LHC. The same parameter set also provides good agreement with the distributions of single leptons from semileptonic heavy flavor decays at RHIC and the LHC. The limit on the width of the uncertainty band is now set by the uncertainty due to bottom quark production and decay.

We have used the same fit parameters in the calculation of J/ψ production in the color evaporation model and have thus provided the first uncertainty band on J/ψ production in this approach. The energy dependence of the total J/ψ cross section that results is a good match to the data up to collider energies. The p_T distributions are also in good agreement with the data from RHIC and the LHC. In future work, we will use our new parameter set to place limits on the contriubtion of B meson decays to J/ψ production and will also study cold nuclear matter effects on J/ψ production.

Acknowledgments

We thank M. Cheng, L. Linden Levy, P. Petreczky, R. Soltz and P. Vranas for discussions. The work of R. V. and R. E. N. was performed under the auspices of the U.S. Department of Energy by Lawrence Livermore National Laboratory under Contract DE-AC52-07NA27344 and was also supported in part by the JET Collaboration.

References

[1] R. Vogt, Eur. Phys. J. ST **155**, 213 (2008) [arXiv:0709.2531 [hep-ph]].
[2] M. Cacciari, P. Nason and R. Vogt, Phys. Rev. Lett. **95**, 122001 (2005).
[3] R. Gavai, D. Kharzeev, H. Satz, G. A. Schuler, K. Sridhar and R. Vogt, Int. J. Mod. Phys. A **10**, 3043 (1995).
[4] C. McNeile, C. T. H. Davies, E. Follana, K. Hornbostel and G. P. Lepage, Phys. Rev. D **82**, 034512 (2010).
[5] C. Lourenço and H. K. Wöhri, Phys. Rept. **433**, 127 (2006) [hep-ph/0609101].
[6] A. Adare *et al.* [PHENIX Collaboration], Phys. Rev. Lett. **97**, 252002 (2006).
[7] Y. Zhang *et al.* [STAR Collaboration], J. Phys. G **38**, 124142 (2011).
[8] L. Adamczyk *et al.* [STAR Collaboration], arXiv:1204.4244 [nucl-ex].
[9] B. Abelev *et al.* [ALICE Collaboration], arXiv:1205.4007 [hep-ex].
[10] B. Abelev *et al.* [ALICE Collaboration], arXiv:1201.3791 [hep-ex].
[11] K. Aamodt *et al.* [ALICE Collaboration], Phys. Lett. B **704**, 011 (2011).
[12] B. Abelev *et al.* [ALICE Collaboration], arXiv:1203.3641 [hep-ex].
[13] P. L. McGaughey, E. Quack, P. V. Ruuskanen, R. Vogt and X.-N. Wang, Int. J. Mod. Phys. A **10**, 2999 (1995).